Simultaneous fit for CGC inclusive DIS and SIHP cross sections

Piotr Korcyl

UNIWERSYTET JAGIELLOŃSKI W KRAKOWIE

in collaboration with H. Le, F. Salazar, and T. Stebel

based on arxiv:2607.xxxxx

Gluon Saturation, Diffraction and Multihadron Production at the EIC: Theory, Simulations and Feasibility of Measurements, Stony Brook University, July 14, 2026

NATIONAL SCIENCE CENTRE POLAND This work is supported by NCN grant nr 2022/46/E/ST2/00346.

Explaining the title

- *CGC*: Color Glass Condensate is an effective description of processes in pp and pA collisions
- *Simultaneous fit*: the goal is to describe simultaneously several sets of experimental data
- *inclusive DIS*: inclusive Deep Inelastic Scattering
- *SIHP*: Single Hadron Inclusive Production

CGC: Color Glass Condensate is an effective description of processes in *pp* and *pA* collisions at high energies $\Longleftrightarrow$ small x

- access to unintegrated parton distribution functions
- nonperturbative initial condition - model
- perturbative evolution equation
- predictions of cross-sections at high-energies/small-x

$\ln Q^2$ and $\ln 1/x$ evolution

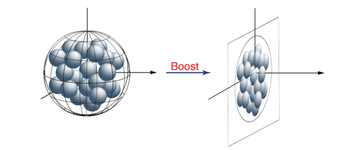

Fig. 2. An ultrarelativistic nucleus appears as a "pancake" with the $A^{1/3}$-enhanced color charge density.

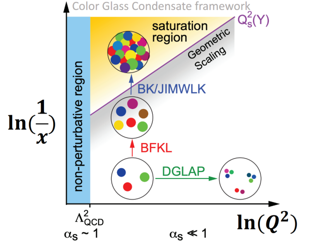

Y. Kovchegov, *Brief Review of Saturation Physics*, Acta Phys. Pol. B, 45 (2014) 2241

Color Glass Condensate framework

Multiple gluon scattering in the Color Glass Condensate (CGC) as a Wilson line operator

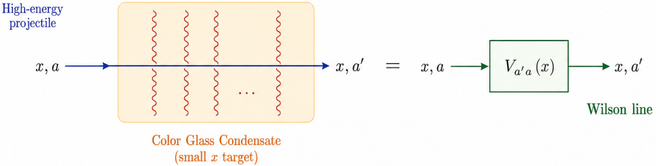

- Eikonal projectile parton (large + momentum)
- Background gluon field of the target (small x)
- Color Glass Condensate: classical color field $A_a^-(x)$
- Eikonal propagation described by Wilson line

Wilson line in the fundamental representation:

$$\boxed{V_x = \mathcal{P}\exp\left[ig\int_{-\infty}^{+\infty} dx^-\, A_a^-(x^-, x_\perp = x)\, t^a\right]}$$

$\mathcal{P}$: path ordering in x^-

t^a: $SU(N_c)$ generators in the fundamental representation

Scattering amplitude: $\boxed{\mathcal{A}(x, a \to x, a') = \left\langle V_{a'a}(x)\right\rangle_Y}$

$\langle\cdots\rangle_Y$: average over target color field configurations with rapidity Y

Color Glass Condensate framework

The distribution of Wilson lines is related to the distribution of color charges in the target.

The expectation value of an operator at the scale Λ^+ is given by

$$\langle \mathscr{O} \rangle_{\Lambda^+} = \int [D\rho] W_{\Lambda^+}[\rho] \mathscr{O}[\rho]$$

where $\mathscr{O}[\rho]$ is the expectation value of the operator for a particular configuration of color charges ρ.

The evolution of $W_{\Lambda^+}[\rho]$ with Λ^+ is governed by the functional JIMWLK equation

$$\frac{\partial W_{\Lambda^+}[\rho]}{\partial \ln(\Lambda^+)} = -\mathscr{H}[\rho, \frac{\delta}{\delta \rho}] W_{\Lambda^+}[\rho],$$

where $\mathscr{H}$ is known as the JIMWLK Hamiltonian.

Inclusive Deep Inealastic Scattering cross section

François Gelis et al.

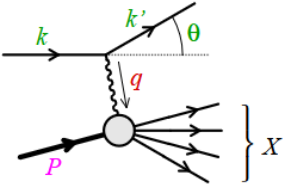

$$s \equiv (P+k)^2$$
$$Q^2 \equiv -q^2$$
$$x \equiv Q^2/2P\cdot q$$
$$xy \equiv Q^2/s$$

Figure 1: *Kinematics of Deep Inelastic Scattering.*

The Color Glass Condensate, F. Gelis, E. Iancu, J. Jalilian-Marian, R. Venugopalan

Inclusive Deep Inealastic Scattering cross section

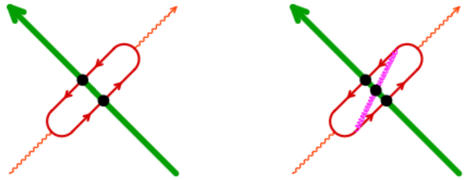

Figure 4: *Left: leading Order (LO) contribution to DIS off the CGC. Right: NLO contribution.*

The Color Glass Condensate, F. Gelis, E. Iancu, J. Jalilian-Marian, R. Venugopalan

$$\sigma_{T,L}(Y,Q^2) = \sigma_0 \sum_f \int_0^1 dz \int d\bar{\boldsymbol{r}}_\perp |\psi^f_{T,L}(e_f, m_f, z, Q^2, \bar{\boldsymbol{r}}_\perp)|^2 N_F(Y, \bar{\boldsymbol{r}}_\perp)$$

where

$$N_F(Y, \bar{\boldsymbol{r}}_\perp) = \frac{1}{N_c} \mathrm{Tr}\left[U_Y(0) U_Y^\dagger(\bar{\boldsymbol{r}}_\perp)\right]$$

JIMWLK equation → BK equation

Numerical solution of the JIMWLK equation that yields the evolution of the distribution of Wilson lines is very demanding.

In the large N_c limit, if only the dipole amplitude is what we need, JIMWLK equation reduces to the BK equation for $N_F(Y, \bar{\boldsymbol{r}}_\perp)$ directly.

Initial condition

$$N_F^{\mathrm{MV}}(Y = Y_0, \bar{\boldsymbol{r}}_\perp) = 1 - \exp\left[-\frac{\left(r^2 Q_0\right)^\gamma}{4} \ln\left(\frac{1}{r\Lambda} + e\right)\right]$$

Goal of the exercise

Test the universality of the CGC approach:

- so far, the fits were performed one observable at a time
- in some works, fitted parameters were used to calculate another observable and compared with experimental data
- we plan to investigate if a simultaneous fit to a set of observables is possible
- on the way, we will develop numerical tools that, unexpectedly, can have more applications and open new opportunities

Single inclusive hadron production in proton-proton collisions

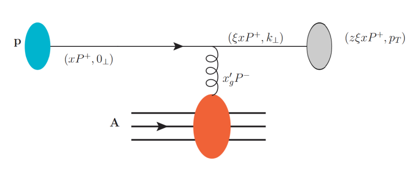

Y. Shi, L. Wang, S. Wei, B. Xiao, Phys. Rev. Lett. 128 (2022) 202302

$$\frac{dN_h}{dy_h d^2p_t} = \frac{\frac{1}{2}\sigma_0}{\sigma_{\rm inel}} \frac{K}{(2\pi)^2} \int_{x_F}^{1} \frac{dz}{z^2} \Big\{ \sum_q \Big[x_1 f_{q/p}(x_1, p_t^2) N_F(x_2, \frac{p_t}{z}) D_{h/q}(z, p_t^2) \Big] + \\ + \Big[x_1 f_{g/p}(x_1, p_t^2) N_A(x_2, \frac{p_t}{z}) D_{h/g}(z, p_t^2) \Big] \Big\}$$

Negatively charged hadron and π^0 yields in proton-proton collisions at $\sqrt{S_{NN}} = 200$ GeV

- probes another type of correlations: N_A
- studied and described in the CGC framework, also at NLO
- K factor needed to account for missing higher-order corrections

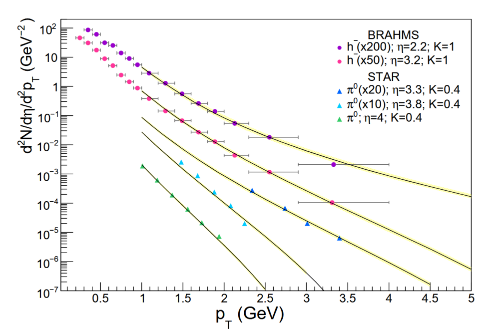

J. Albacete, C. Marquet, *Single inclusive hadron production at RHIC and the LHC from the Color Glass Condensate*, Phys.Lett.B687:174-179,2010

Simultaneous fit for CGC inclusive DIS and SIHP cross sections

Framework: requirements

- evolution equation
- initial condition
- access to the gluon dipole amplitude in position and momentum spaces
- minimization algorithm $\Rightarrow$ levmar library
- access to fragmentation functions and PDFs $\Rightarrow$ LHAPDF library

Framework: features

- BK evolution equation with kinematical constraint
- Balitsky/daughter/mother dipole prescription for the running coupling
- Euler/Runge integration scheme
- uncertainty estimation
- parallelization $\Rightarrow$ shorter running time
- ...

Balitsky-Kovchegov evolution equation

The LO BK equation reads

$$\frac{\partial S_{\bar{\boldsymbol{x}}_\perp \bar{\boldsymbol{y}}_\perp}(\eta)}{\partial \eta} = \frac{\bar{\alpha}_s}{2\pi} \int d^2 \bar{\boldsymbol{z}}_\perp \; \mathscr{M}_{\bar{\boldsymbol{x}}_\perp \bar{\boldsymbol{y}}_\perp \bar{\boldsymbol{z}}_\perp} \left[S_{\bar{\boldsymbol{x}}_\perp \bar{\boldsymbol{z}}_\perp}(\eta) S_{\bar{\boldsymbol{z}}_\perp \bar{\boldsymbol{y}}_\perp}(\eta) - S_{\bar{\boldsymbol{x}}_\perp \bar{\boldsymbol{y}}_\perp}(\eta) \right],$$

where

$$\mathscr{M}_{\bar{\boldsymbol{x}}_\perp \bar{\boldsymbol{y}}_\perp \bar{\boldsymbol{z}}_\perp} = \frac{(\bar{\boldsymbol{x}}_\perp - \bar{\boldsymbol{y}}_\perp)^2}{(\bar{\boldsymbol{x}}_\perp - \bar{\boldsymbol{z}}_\perp)^2 (\bar{\boldsymbol{z}}_\perp - \bar{\boldsymbol{y}}_\perp)^2}.$$

Rewritten in radial variables

$$\frac{\partial S(r,\eta)}{\partial \eta} = \frac{\bar{\alpha}_s}{2\pi} \int d\phi \, dr_z \, r_z \, \frac{r^2}{r_z^2 (r^2 + r_z^2 - 2 r r_z \cos\phi)} \times \\ \times \left[S(r_z, \eta) \, S\left(\sqrt{r^2 + r_z^2 - 2 r r_z \cos\phi}, \eta \right) - S(r,\eta) \right].$$

Balitsky-Kovchegov evolution equation

Account for several additional physical effects, such as the running of the coupling constant with the energy scale, resummation of subleading corrections

$$\frac{\partial S(r,\eta)}{\partial \eta} = \int d\phi \, dr_z \, r_z \times$$
$$\times \left[\frac{\bar{\alpha}_s(r)}{2\pi r_z^2} \left(\frac{r^2}{r_{zy}^2 + \varepsilon^2} + \frac{\bar{\alpha}_s(r_z)}{\bar{\alpha}_s(r_{zy})} - 1 + \frac{r_z^2}{r_{zy}^2 + \varepsilon^2} \left(\frac{\bar{\alpha}_s(r_{zy})}{\bar{\alpha}_s(r_z)} - 1 \right) \right) \right] \times$$
$$\times \left[S(r_z, \eta - \delta_{r_z;r}) S(r_{zy}, \eta - \delta_{r_{zy};r}) - S(r,\eta) \right],$$

where $r_{zy} = \sqrt{r^2 + r_z^2 - 2 r r_z \cos\phi}$. The shifts in η in the dipole amplitudes are given by $\delta_{r_z;r} = \max\left\{0, 2\log\frac{r}{r_z}\right\}$ and similarly $\delta_{r_{zy};r} = \max\left\{0, 2\log\frac{r}{r_{zy}}\right\}$.

B. Ducloué, E. Iancu, G. Soyez, D.N. Triantafyllopoulos, *HERA data and collinearly-improved BK dynamics*, Phys.Lett.B 803 (2020) 135305

Framework: features

- automatic differentiation
  - improves the convergence of the minimization algorithm
  - gives access to the Hessian matrix
- logarithmic Fourier Transform
  - uses standard FFTW 1D Fourier transform, but works on a logarithmic radial grid
  - can be implemented using automatic differentiation
- Monte Carlo Bayesian inference for uncertainty estimation
  - provides uncertainty estimates even for non-Gaussian distributions
  - can be cross-checked with the Hessian method

Automatic Differentiation for the Balitsky-Kovchegov evolution equation

$$S(r,\eta) \to \begin{pmatrix} S(r,\eta) \\ \partial_{Q_0} S(r,\eta) \\ \partial_\gamma S(r,\eta) \\ \partial^2_{Q_0} S(r,\eta) \\ \partial^2_\gamma S(r,\eta) \\ \partial_{Q_0}\partial_\gamma S(r,\eta) \end{pmatrix}$$

$$\frac{\partial S(r,\eta)}{\partial \eta} = \int d\phi\, dr_z\, r_z \times$$
$$\times \left[\frac{\bar{\alpha}_s(r)}{2\pi r_z^2} \left(\frac{r^2}{r_{zy}^2+\varepsilon^2} + \frac{\bar{\alpha}_s(r_z)}{\bar{\alpha}_s(r_{zy})} - 1 + \frac{r_z^2}{r_{zy}^2+\varepsilon^2} \left(\frac{\bar{\alpha}_s(r_{zy})}{\bar{\alpha}_s(r_z)} - 1 \right) \right) \right] \times$$
$$\times \left[S(r_z, \eta - \delta_{r_z;r}) S(r_{zy}, \eta - \delta_{r_{zy};r}) - S(r,\eta) \right],$$

gives $S(r,\eta)$ together with the evolved derivatives.

F. Cougoulic, P. Korcyl, T. Stebel, *Improving the solver for the Balitsky-Kovchegov evolution equation with Automatic Differentiation*, Comput.Phys.Commun. 313 (2025) 109616

Results

Scheme	Q^2_{s0} (GeV^2)	γ	C^2	$\sigma_0/2$ (mb)	K-RHIC	K-LHCb
rcBK	0.1411(36)	1.1521(77)	10.3(1.1)	17.26(28)	—	—
kcBK	0.1084(27)	1.1135(73)	1.276(68)	19.69(31)	—	—
rcBK	0.1483(34)	1.1661(74)	8.69(85)	16.79(24)	5.61(48)	2.990(93)
kcBK	0.1163(26)	1.1310(71)	1.133(54)	18.94(27)	6.08(51)	3.292(10)

Table: Best-fit parameters. The first and second rows provide the baseline fit to DIS data only, while subsequent rows show the results of the global fit.

Scheme	$\chi^2_{\rm DIS}/\mathrm{d.o.f}$	$\chi^2_{\rm RHIC}/\mathrm{d.o.f}$	$\chi^2_{\rm LHC}/\mathrm{d.o.f}$	$\chi^2_{\rm tot}/\mathrm{d.o.f}$
rcBK	0.97	—	—	0.975
kcBK	1.12	—	—	1.132
rcBK	0.98	0.21	0.94	**0.943**
kcBK	1.14	0.2	1.29	1.139

Table: χ^2 values for various schemes.

Simultaneous fit for CGC inclusive DIS and SIHP cross sections

Details

Uncertainties

- account for the theoretical uncertainty in the SIHP due to the scale variation
- account for the statistical uncertainty of the fragmentation function
- account for the statistical uncertainty of the parton distribution function

Scale variation:

- tested various definitions of the factorization scale for the fragmentation function: parton momentum, hadron momentum, ect.

Fragmentation function sets

- tested various sets of fragmentation functions and PDFs

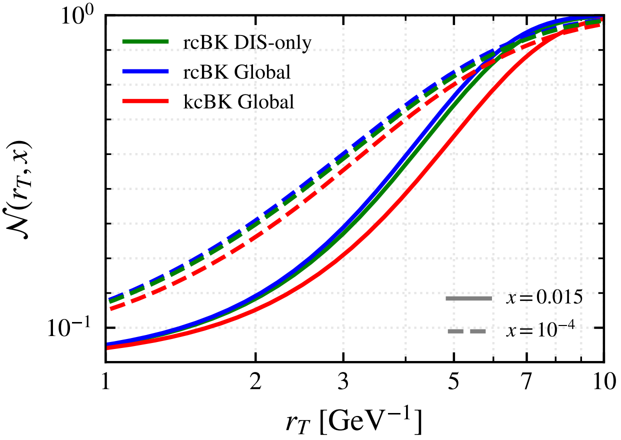
rcBK DIS-only
rcBK Global
kcBK Global
$x = 0.015$
$x = 10^{-4}$
10^0
10^{-1}
$\mathcal{N}(r_T, x)$
1
2
3
5
7
10
r_T [GeV^{-1}]

Inclusive DIS data from HERA

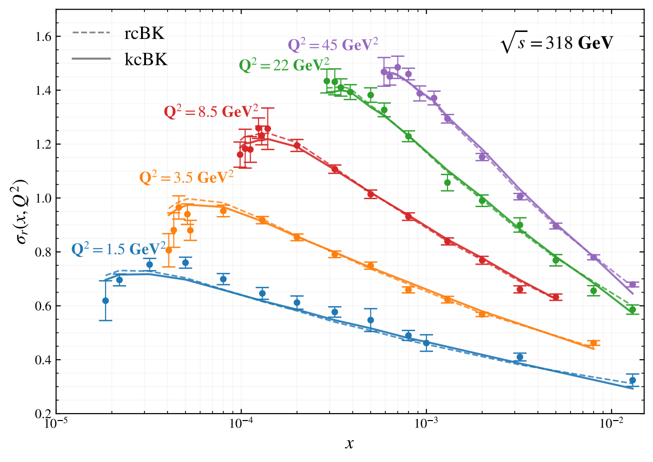

Simultaneous fit for CGC inclusive DIS and SIHP cross sections

SIHP from RHIC

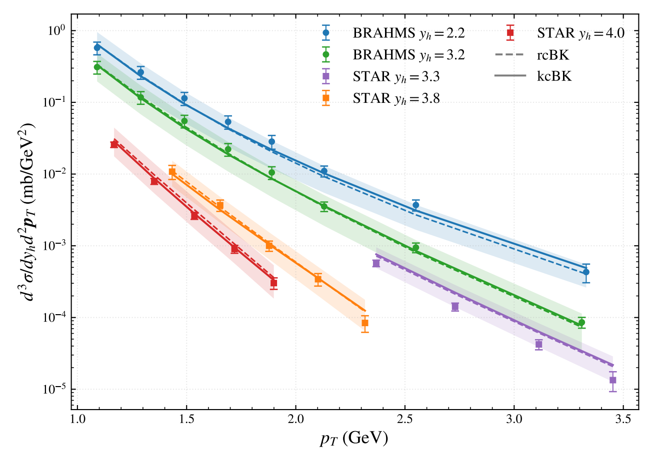

Simultaneous fit for CGC inclusive DIS and SIHP cross sections

SIHP from LHC

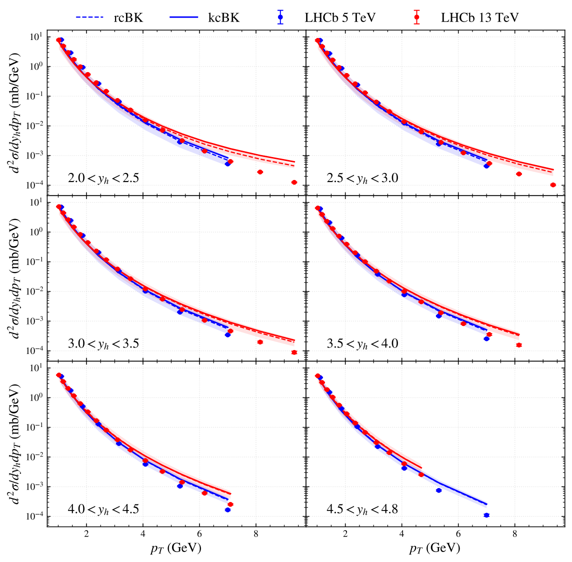

Uncertainties obtained using the Hessian matrix

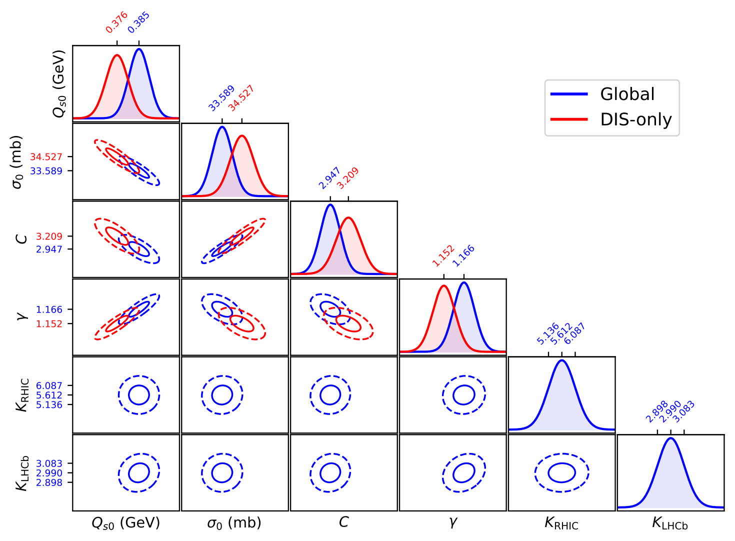

Simultaneous fit for CGC inclusive DIS and SIHP cross sections

Check of the validity of MC Bayesian inference approach

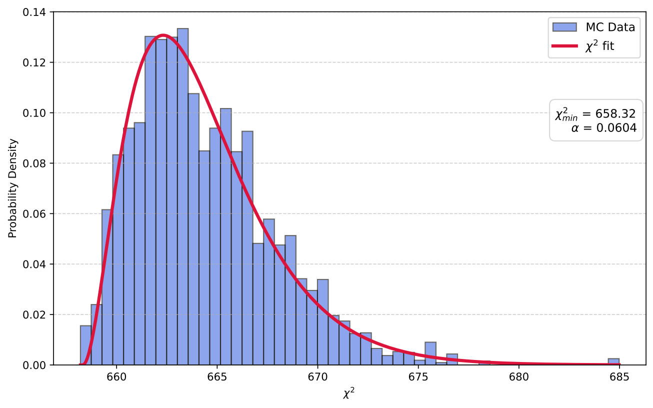

Simultaneous fit for CGC inclusive DIS and SIHP cross sections

Comparison of MC Bayesian inference vs. Hessian method

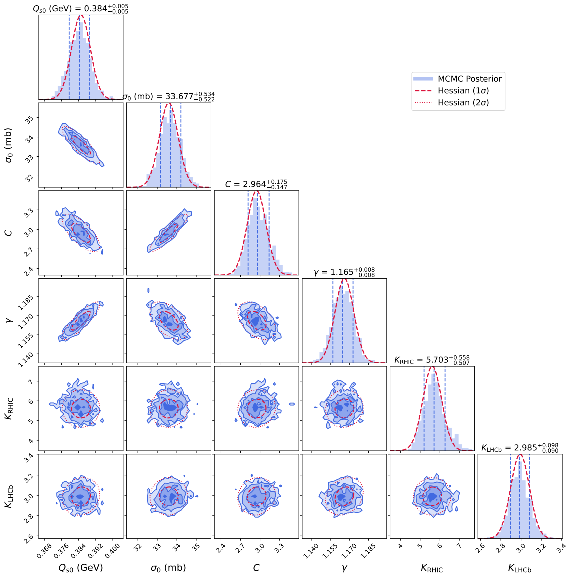

Fragmentation function sets

FFs	Q range (GeV)	x limits
NNFF1.0 (LO)	$1 - 10000$	$0.01 - 1$
JAM19 (NLO)	$1.14 - 316$	$10^{-6} - 1$
DSS (LO)	$1 - 316.23$	$0.01 - 1$
NPC23 (NLO)	$4 - 4000$	$0.003 - 1$

Table: Kinematical boundaries of the fragmentation function sets tested in this work.

Fragmentation function sets

<table>
<tr><th>FFs</th><th>Q_{s0}^2</th><th>$\sigma_0/2$</th><th>C^2</th><th>γ</th><th>K_{BRAHMS}</th><th>K_{STAR}</th><th>K_{LHCb5}</th><th>K_{LHCb13}</th></tr>
<tr><td rowspan="2">NNFF1.0</td><td rowspan="2">0.15</td><td rowspan="2">16.8</td><td rowspan="2">8.7</td><td rowspan="2">1.166</td><td colspan="2">5.612</td><td colspan="2">2.99</td></tr>
<tr><td>0.156</td><td>0.266</td><td>0.805</td><td>1.003</td></tr>
<tr><td rowspan="2">NNFF1.0</td><td rowspan="2">0.15</td><td rowspan="2">16.8</td><td rowspan="2">8.6</td><td rowspan="2">1.167</td><td>6.484</td><td>4.646</td><td colspan="2">2.995</td></tr>
<tr><td>0.064</td><td>0.109</td><td>0.802</td><td>1.006</td></tr>
<tr><td rowspan="2">JAM19</td><td rowspan="2">0.18</td><td rowspan="2">15.1</td><td rowspan="2">4.6</td><td rowspan="2">1.217</td><td>4.987</td><td>2.938</td><td colspan="2">2.08</td></tr>
<tr><td>0.385</td><td>0.045</td><td>2.221</td><td>5.074</td></tr>
<tr><td rowspan="2">DSS</td><td rowspan="2">0.17</td><td rowspan="2">15.7</td><td rowspan="2">5.8</td><td rowspan="2">1.2</td><td>4.418</td><td>2.361</td><td colspan="2">1.834</td></tr>
<tr><td>0.338</td><td>0.043</td><td>1.323</td><td>3.431</td></tr>
<tr><td rowspan="2">NPC23</td><td rowspan="2">0.20</td><td rowspan="2">14.0</td><td rowspan="2">3.0</td><td rowspan="2">1.272</td><td>14.945</td><td>4.332</td><td colspan="2">6.024</td></tr>
<tr><td>1.1</td><td>0.444</td><td>8.102</td><td>9.804</td></tr>
<tr><td rowspan="2">NPC23 $p_T \leq 6$</td><td rowspan="2">0.16</td><td rowspan="2">16.3</td><td rowspan="2">7.5</td><td rowspan="2">1.188</td><td>14.208</td><td>4.583</td><td colspan="2">6.416</td></tr>
<tr><td>0.391</td><td>0.672</td><td>6.48</td><td>4.949</td></tr>
</table>

Table: Results for different choices of the fragmentation function sets. The results obtained with the NPC23 set differ significantly from the other choices; in particular, the values of the K factors are larger.

Fragmentation function sets

FFs	χ^2_{DIS}/dof	χ^2/dof
NNFF1.0	0.975	0.943
NNFF1.0	0.976	0.939
JAM19	1.126	1.706
DSS	1.049	1.363
NPC23	1.390	2.975
NPC23 $p_T \leq 6$	1.005	1.786

Table: Results for different choices of the fragmentation function sets. The results obtained with the NPC23 set differ significantly from the other choices; in particular, the values of the K factors are larger.

Fragmentation function sets

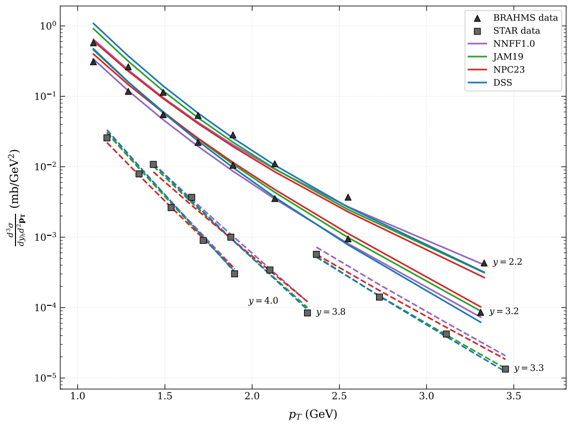

Figure: Results for different sets of fragmentation functions (FFs) using the CTEQ PDF based on the best fit: RHIC data.

Fragmentation function sets

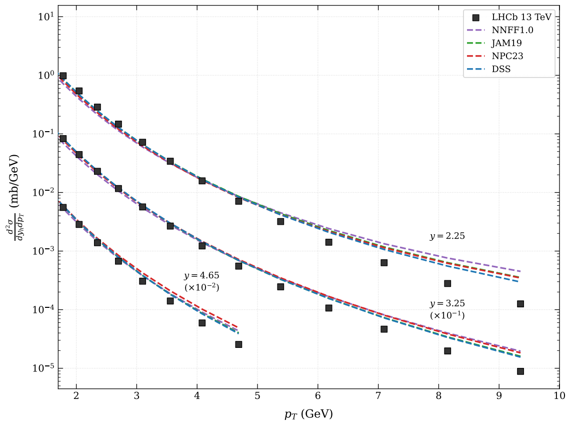

Figure: Results for different sets of fragmentation functions (FFs) using the CTEQ PDF based on the best fit: selected experimental data points for LHCb 13 TeV data.

Summary

- we have developed a framework that allows for an efficient fitting of several observables within the CGC approach
- we performed a combined description of inclusive DIS and single inclusive hadron production cross-sections
- the LO framework provides a reasonable description; tensions can be addressed by higher-order corrections
- single inclusive hadron production sensitive to the choice of the fragmentation function sets
- future steps:
  - NLO BK
  - inclusion of heavy ions
  - solutions with the full JIMWLK evolution equation

Thank you very much for your attention!